



HAL
open science

Unphysical Discontinuities, Intruder States and Regularization in GW Methods

Enzo Monino, Pierre-Francois Loos

► **To cite this version:**

Enzo Monino, Pierre-Francois Loos. Unphysical Discontinuities, Intruder States and Regularization in GW Methods. *Journal of Chemical Physics*, 2022, 156 (23), pp.231101. 10.1063/5.0089317. hal-03586690

HAL Id: hal-03586690

<https://hal.science/hal-03586690>

Submitted on 24 Feb 2022

HAL is a multi-disciplinary open access archive for the deposit and dissemination of scientific research documents, whether they are published or not. The documents may come from teaching and research institutions in France or abroad, or from public or private research centers.

L'archive ouverte pluridisciplinaire **HAL**, est destinée au dépôt et à la diffusion de documents scientifiques de niveau recherche, publiés ou non, émanant des établissements d'enseignement et de recherche français ou étrangers, des laboratoires publics ou privés.

Unphysical Discontinuities, Intruder States and Regularization in GW Methods

Enzo Monino¹ and Pierre-François Loos^{1, a)}

Laboratoire de Chimie et Physique Quantiques (UMR 5626), Université de Toulouse, CNRS, UPS, France

By recasting the non-linear frequency-dependent GW quasiparticle equation into a linear eigenvalue problem, we explain the appearance of multiple solutions and unphysical discontinuities in various physical quantities computed within the GW approximation. Considering the GW self-energy as an effective Hamiltonian, it is shown that these issues are key signatures of strong correlation in the $(N \pm 1)$ -electron states and can be directly related to the intruder state problem. A simple and efficient regularization procedure inspired by the similarity renormalization group is proposed to avoid such issues and speed up convergence of partially self-consistent GW calculations.

I. INTRODUCTION

The GW approximation of many-body perturbation theory^{1,2} allows to compute accurate charged excitation (*i.e.*, ionization potentials, electron affinities and fundamental gaps) in solids and molecules.³⁻⁶ Its popularity in the molecular electronic structure community is rapidly growing⁷⁻²⁹ thanks to its relatively low computational cost³⁰⁻³⁴ and somehow surprising accuracy for weakly-correlated systems.^{19-21,29,35,36}

The idea behind the GW approximation is to recast the many-body problem into a set of non-linear one-body equations. The introduction of the self-energy Σ links the non-interacting Green's function G_0 to its fully-interacting version G via the following Dyson equation:

$$G = G_0 + G_0 \Sigma G \quad (1)$$

Electron correlation is then explicitly incorporated into one-body quantities via a sequence of self-consistent steps known as Hedin's equations.¹

In recent studies,³⁷⁻⁴¹ we discovered that one can observe (unphysical) irregularities and/or discontinuities in the energy surfaces of several key quantities (ionization potential, electron affinity, fundamental and optical gaps, total and correlation energies, as well as excitation energies) even in the weakly-correlated regime. These issues were discovered in Ref. 37 while studying a model two-electron system⁴²⁻⁴⁴ and they were further investigated in Ref. 38, where we provided additional evidences and explanations of these undesirable features in real molecular systems. In particular, we showed that each branch of the self-energy Σ is associated with a distinct quasiparticle solution, and that each switch between solutions implies a significant discontinuity in the quasiparticle energy due to the transfer of weight between two solutions of the quasiparticle equation.³⁸ Multiple solution issues in GW appears frequently,^{20,22,45} especially for orbitals that are energetically far from the Fermi level, such as in core ionized states.^{46,47}

In addition to obvious irregularities in potential energy surfaces that hampers the accurate determination of properties such as equilibrium bond lengths and harmonic vibrational frequencies,^{39,40} one direct consequence of these discontinuities is the difficulty to converge (partially) self-consistent GW calculations as the self-consistent procedure jumps erratically

from one solution to the other even if convergence accelerator techniques such as DIIS are employed.^{38,48,49} Note in passing that the present issues do not only appear in GW as the T -matrix⁵⁰⁻⁵³ and second-order Green's function (or second Born) formalisms⁵⁴⁻⁶⁴ exhibit the same drawbacks.

It was shown that these problems can be tamed by using a static Coulomb-hole plus screened-exchange (COHSEX)^{1,65-67} self-energy⁴⁰ or by considering a fully self-consistent GW scheme,^{14,32,68-74} where one considers not only the quasiparticle solution but also the satellites at each iteration.⁴¹ However, none of these solutions is completely satisfying as a static approximation of the self-energy can induce significant loss in accuracy and fully self-consistent calculations can be quite challenging in terms of implementation and cost.

In the present article, via an unfolding process of the non-linear GW equation,⁷⁵ we provide further physical insights into the origin of these discontinuities by highlighting, in particular, the role of intruder states. Inspired by regularized electronic structure theories,^{76,77} these new insights allow us to propose a cheap and efficient regularization scheme in order to avoid these issues and speed up convergence of partially self-consistent GW calculations.

Here, for the sake of simplicity, we consider the one-shot G_0W_0 ^{65,78-85} but the same analysis can be performed in the case of (partially) self-consistent schemes such as $evGW$ ^{65,85-88} (where one updates only the quasiparticle energies) and $qsGW$ ^{7,89-93} (where both quasiparticle energies and orbitals are updated at each iteration). Moreover, we consider a Hartree-Fock (HF) starting point but it can be straightforwardly extended to a Kohn-Sham starting point. Throughout this article, p and q are general (spatial) orbitals, i, j, k , and l denotes occupied orbitals, a, b, c , and d are vacant orbitals, while m labels single excitations $i \rightarrow a$. Atomic units are used throughout.

II. DOWNFOLDING: THE NON-LINEAR GW PROBLEM

Within the G_0W_0 approximation, in order to obtain the quasiparticle energies and the corresponding satellites, one solve, for each spatial orbital p , the following (non-linear) quasiparticle equation

$$\epsilon_p^{\text{HF}} + \Sigma_p^c(\omega) - \omega = 0 \quad (2)$$

where ϵ_p^{HF} is the p th HF orbital energy and the correlation part of the G_0W_0 self-energy is constituted by a hole (h) and a

^{a)}Electronic mail: loos@irsamc.ups-tlse.fr

particle (p) term as follows

$$\Sigma_p^c(\omega) = \sum_{im} \frac{2(pi|m)^2}{\omega - \epsilon_i^{\text{HF}} + \Omega_m^{\text{RPA}}} + \sum_{am} \frac{2(pa|m)^2}{\omega - \epsilon_a^{\text{HF}} - \Omega_m^{\text{RPA}}} \quad (3)$$

Within the Tamm-Dancoff approximation (that we enforce here for the sake of simplicity), the screened two-electron integrals are given by

$$(pq|lm) = \sum_{ia} (pq|ia) X_{ia,m}^{\text{RPA}} \quad (4)$$

where Ω_m^{RPA} and X_m^{RPA} are respectively the m th eigenvalue and eigenvector of the random-phase approximation (RPA) problem, *i.e.*,

$$\mathbf{A}^{\text{RPA}} \cdot \mathbf{X}_m^{\text{RPA}} = \Omega_m^{\text{RPA}} \mathbf{X}_m^{\text{RPA}} \quad (5)$$

with

$$A_{ia,jb}^{\text{RPA}} = (\epsilon_a^{\text{HF}} - \epsilon_i^{\text{HF}}) \delta_{ij} \delta_{ab} + (ia|bj) \quad (6)$$

and

$$(pq|ia) = \iint \phi_p(\mathbf{r}_1) \phi_q(\mathbf{r}_1) \frac{1}{|\mathbf{r}_1 - \mathbf{r}_2|} \phi_i(\mathbf{r}_2) \phi_a(\mathbf{r}_2) d\mathbf{r}_1 d\mathbf{r}_2 \quad (7)$$

are two-electron integrals over the HF (spatial) orbitals $\phi_p(\mathbf{r})$. Because one must compute all the RPA eigenvalues and eigenvectors to construct the self-energy (3), the computational cost is $O(O^3 V^3) = O(K^6)$, where O and V are the number of occupied and virtual orbitals, respectively, and $K = O + V$ is the total number of orbitals.

As a non-linear equation, Eq. (2) has many solutions $\epsilon_{p,s}^{\text{GW}}$ and their corresponding weights are given by the value of the following renormalization factor

$$0 \leq Z_{p,s} = \left[1 - \left. \frac{\partial \Sigma_p^c(\omega)}{\partial \omega} \right|_{\omega=\epsilon_{p,s}^{\text{GW}}} \right]^{-1} \leq 1 \quad (8)$$

In a well-behaved case, one of the solution (the so-called quasiparticle) ϵ_p^{GW} has a large weight Z_p . Note that we have the following important conservation rules^{94–96}

$$\sum_s Z_{p,s} = 1 \quad \sum_s Z_{p,s} \epsilon_{p,s}^{\text{GW}} = \epsilon_p^{\text{HF}} \quad (9)$$

which physically shows that the mean-field solution of unit weight is “scattered” by the effect of correlation in many solutions of smaller weights.

III. UPFOLDING: THE LINEAR GW PROBLEM

The non-linear quasiparticle equation (2) can be *exactly* transformed into a larger linear problem via an unfolding process where the 2h1p and 2p1h sectors are unfolded from the 1h and 1p sectors.^{75,97–100} For each orbital p , this yields a linear eigenvalue problem of the form

$$\mathbf{H}^{(p)} \cdot \mathbf{c}^{(p,s)} = \epsilon_{p,s}^{\text{GW}} \mathbf{c}^{(p,s)} \quad (10)$$

with

$$\mathbf{H}^{(p)} = \begin{pmatrix} \epsilon_p^{\text{HF}} & \mathbf{V}_p^{2\text{h1p}} & \mathbf{V}_p^{2\text{p1h}} \\ (\mathbf{V}_p^{2\text{h1p}})^\top & \mathbf{C}^{2\text{h1p}} & \mathbf{0} \\ (\mathbf{V}_p^{2\text{p1h}})^\top & \mathbf{0} & \mathbf{C}^{2\text{p1h}} \end{pmatrix} \quad (11)$$

where

$$C_{ija,kcl}^{2\text{h1p}} = [(\epsilon_i^{\text{HF}} + \epsilon_j^{\text{HF}} - \epsilon_a^{\text{HF}}) \delta_{jl} \delta_{ac} - 2(ja|cl)] \delta_{ik} \quad (12)$$

$$C_{iab,kcd}^{2\text{p1h}} = [(\epsilon_a^{\text{HF}} + \epsilon_b^{\text{HF}} - \epsilon_i^{\text{HF}}) \delta_{ik} \delta_{ac} + 2(ai|kc)] \delta_{bd} \quad (13)$$

and the corresponding coupling blocks read

$$V_{p,klc}^{2\text{h1p}} = \sqrt{2}(pk|cl) \quad V_{p,kcd}^{2\text{p1h}} = \sqrt{2}(pd|kc) \quad (14)$$

The size of this eigenvalue problem is $1 + O^2 V + OV^2 = O(K^3)$, and it has to be solved for each orbital that one wishes to correct. Thus, this step scales as $O(K^9)$ with conventional diagonalization algorithms. Note, however, that the blocks $\mathbf{C}^{2\text{h1p}}$ and $\mathbf{C}^{2\text{p1h}}$ do not need to be recomputed for each orbital.

It is crucial to understand that diagonalizing $\mathbf{H}^{(p)}$ [see Eq. (11)] is completely equivalent to solving the quasiparticle equation (2). This can be further illustrated by expanding the secular equation associated with Eq. (11)

$$\det[\mathbf{H}^{(p)} - \omega \mathbf{1}] = 0 \quad (15)$$

and comparing it with Eq. (2) by setting

$$\Sigma_p^c(\omega) = \mathbf{V}_p^{2\text{h1p}} \cdot (\omega \mathbf{1} - \mathbf{C}^{2\text{h1p}})^{-1} \cdot (\mathbf{V}_p^{2\text{h1p}})^\top + \mathbf{V}_p^{2\text{p1h}} \cdot (\omega \mathbf{1} - \mathbf{C}^{2\text{p1h}})^{-1} \cdot (\mathbf{V}_p^{2\text{p1h}})^\top \quad (16)$$

where $\mathbf{1}$ is the identity matrix. Because the renormalization factor (8) corresponds to the projection of the vector $\mathbf{c}^{(p,s)}$ onto the reference (or internal) space, the weight of a solution (p, s) is given by the first coefficient of their corresponding eigenvector $\mathbf{c}^{(p,s)}$, *i.e.*,

$$Z_{p,s} = [c_1^{(p,s)}]^2 \quad (17)$$

One can see this downfolding process as the construction of a frequency-dependent effective Hamiltonian where the internal space is composed by a single Slater determinant of the 1h or 1p sector and the external (or outer) space by all the 2h1p and 2p1h configurations.^{75,101,102} The main mathematical difference between the two approaches is that, by diagonalizing Eq. (11), one has directly access to the internal and external components of the eigenvectors associated with each quasiparticle and satellite, and not only their projection in the reference space as shown by Eq. (17).

The element ϵ_p^{HF} of $\mathbf{H}^{(p)}$ [see Eq. (11)] corresponds to the (approximate) relative energy of the $(N \pm 1)$ -electron reference determinant (compared to the N -electron HF determinant) while the eigenvalues of the blocks $\mathbf{C}^{2\text{h1p}}$ and $\mathbf{C}^{2\text{p1h}}$, which are $\epsilon_i^{\text{HF}} - \Omega_m^{\text{RPA}}$ and $\epsilon_a^{\text{HF}} + \Omega_m^{\text{RPA}}$ respectively, provide an estimate of the relative energy of the 2h1p and 2p1h determinants. In some situations, one (or several) of these determinants from

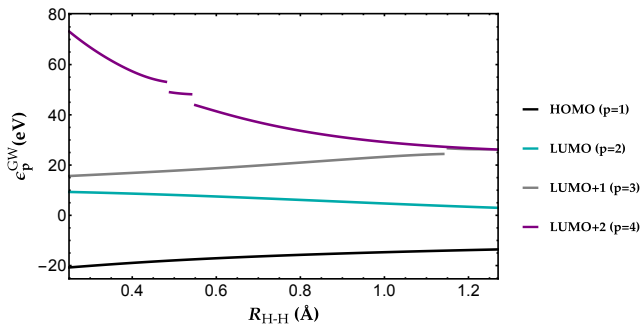


FIG. 1. Quasiparticle energies ϵ_p^{GW} as functions of the internuclear distance R_{H-H} (in Å) of H_2 at the $G_0W_0@HF/6-31G$ level.

the external space may become of similar energy than the reference determinant, resulting in a vanishing denominator in the self-energy (3). Hence, these two diabatic electronic configurations may cross and form an avoided crossing, and this outer-space determinant may be labeled as an intruder state. As we shall see below, discontinuities, which are ubiquitous in molecular systems, arise in such scenarios.

IV. AN ILLUSTRATIVE EXAMPLE

In order to illustrate the appearance and the origin of these multiple solutions, we consider the hydrogen molecule in the 6-31G basis set which corresponds to a two-electron system with four spatial orbitals (one occupied and three virtuals). This example was already considered in our previous work³⁸ but here we provide further insights on the origin of the appearances of these discontinuities. The downfolded and upfolded G_0W_0 schemes have been implemented in the electronic structure package QuAcK¹⁰³ which is freely available at <https://github.com/pfloos/QuAcK>. These calculations are based on restricted HF eigenvalues and orbitals. We denote as $|1\bar{1}\rangle$ the N -electron ground-state Slater determinant where the orbital 1 is occupied by one spin-up and one spin-down electron. Similar notations will be employed for the $(N \pm 1)$ -electron configurations.

In Fig. 1, we report the variation of the quasiparticle energies of the four orbitals as functions of the internuclear distance R_{H-H} . One can easily diagnose two problematic regions showing obvious discontinuities around $R_{H-H} = 1.2$ Å for the LUMO+1 ($p = 3$) and $R_{H-H} = 0.5$ Å for the LUMO+2 ($p = 4$). As thoroughly explained in Ref. 38, if one relies on the linearization of the quasiparticle equation (2) to compute the quasiparticle energies, *i.e.*, $\epsilon_p^{GW} \approx \epsilon_p^{HF} + Z_p \Sigma_p^c(\epsilon_p^{HF})$, these discontinuities are transformed into irregularities as the renormalization factor cancels out the singularities of the self-energy.

Figure 2 shows the evolution of the quasiparticle energy, the energetically close-by satellites and their corresponding weights as functions of R_{H-H} . Let us first look more closely at the region around $R_{H-H} = 1.2$ Å involving the LUMO+1 (left panel of Fig. 2). As one can see, an avoided crossing is formed between two solutions of the quasiparticle equation ($s = 4$ and

$s = 5$). Inspection of their corresponding eigenvectors reveals that the $(N + 1)$ -electron determinants principally involved are the reference 1p determinant $|1\bar{1}3\rangle$ and an excited $(N + 1)$ -electron determinant of configuration $|12\bar{2}\rangle$ that becomes lower in energy than the reference determinant for $R_{H-H} > 1.2$ Å. By construction, the quasiparticle solution diabatically follows the reference determinant $|1\bar{1}3\rangle$ through the avoided crossing (thick lines in Fig. 2) which is precisely the origin of the energetic discontinuity.

A similar scenario is at play in the region around $R_{H-H} = 0.5$ Å for the LUMO+2 (right panel of Fig. 2) but it now involves three solutions ($s = 5$, $s = 6$, and $s = 7$). The electronic configurations of the Slater determinant involved are the $|1\bar{1}4\rangle$ reference determinant as well as two external determinants of configuration $|1\bar{2}3\rangle$ and $|12\bar{3}\rangle$. These states form two avoided crossings in rapid successions, which create two discontinuities in the energy surface (see Fig. 1). In this region, although the ground-state wave function is well described by the N -electron HF determinant, a situation that can be safely labeled as single-reference, one can see that the $(N + 1)$ -electron wave function involves three Slater determinants and can then be labeled as a multi-reference (or strongly-correlated) situation with near-degenerate electronic configurations. Therefore, one can conclude that this downfall of GW is a key signature of strong correlation in the $(N \pm 1)$ -electron states that yields a significant redistribution of weights amongst electronic configurations.

V. INTRODUCING REGULARIZED GW METHODS

One way to alleviate the issues discussed above and to massively improve the convergence properties of self-consistent GW calculations is to resort to a regularization of the self-energy without altering too much the quasiparticle energies.

From a general perspective, a regularized GW self-energy reads

$$\begin{aligned} \tilde{\Sigma}_p^c(\omega; \eta) = & \sum_{im} 2(pi|m)^2 f_\eta(\omega - \epsilon_i^{HF} + \Omega_m^{RPA}) \\ & + \sum_{am} 2(pa|m)^2 f_\eta(\omega - \epsilon_a^{HF} - \Omega_m^{RPA}) \end{aligned} \quad (18)$$

where various choices for the “regularizer” f_η are possible. The main purpose of f_η is to ensure that $\tilde{\Sigma}_p^c(\omega; \eta)$ remains finite even if one of the denominators goes to zero. The regularized solutions $\tilde{\epsilon}_{p,s}^{GW}$ are then obtained by solving the following regularized quasiparticle equation:

$$\epsilon_p^{HF} + \tilde{\Sigma}_p^c(\omega; \eta) - \omega = 0 \quad (19)$$

The most common and well-established way of regularizing Σ is via the simple regularizer $f_\eta(\Delta) = (\Delta \pm \eta)^{-1}$, a strategy somehow related to the imaginary shift used in multi-configurational perturbation theory.¹⁰⁴ Other choices are legitimate like the regularizers considered by Head-Gordon and coworkers within orbital-optimized second-order Møller-Plesset theory.^{76,105}

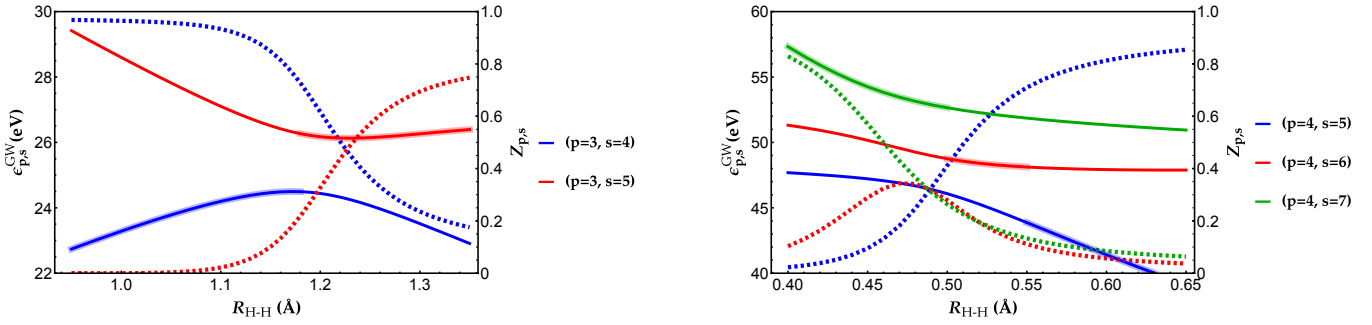


FIG. 2. Selection of quasiparticle and satellite energies $\epsilon_{p,s}^{GW}$ (solid lines) and their renormalization factor $Z_{p,s}$ (dashed lines) as functions of the internuclear distance R_{H-H} (in Å) for the LUMO+1 ($p=3$) and LUMO+2 ($p=4$) orbitals of H_2 at the $G_0W_0@HF/6-31G$ level. The quasiparticle solution (which corresponds to the solution with the largest weight) is represented as a thicker line.

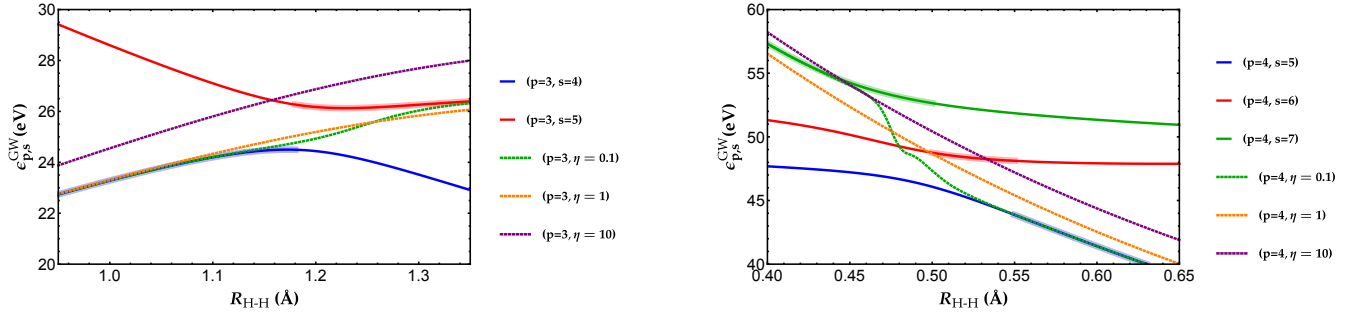


FIG. 3. Comparison between non-regularized (solid lines) and regularized (dashed lines) energies as functions of the internuclear distance R_{H-H} (in Å) for the LUMO+1 ($p=3$) and LUMO+2 ($p=4$) orbitals of H_2 at the $G_0W_0@HF/6-31G$ level. The quasiparticle solution is represented as a thicker line.

Our investigations have shown that the following regularizer

$$f_{\eta}(\Delta) = \frac{1 - e^{-2\Delta^2/\eta^2}}{\Delta} \quad (20)$$

derived from the (second-order) perturbative analysis of the similarity renormalization group equations¹⁰⁶⁻¹⁰⁸ by Evangelista¹⁰⁹ is particularly convenient and effective in the present context. Increasing η gradually integrates out states with denominators Δ larger than η while the states with $\Delta \ll \eta$ are not decoupled from the reference space, hence avoiding intruder state problems.¹¹⁰ Of course, by construction, we have

$$\lim_{\eta \rightarrow 0} \tilde{\Sigma}_p^c(\omega; \eta) = \Sigma_p^c(\omega) \quad (21)$$

Figure 3 compares the non-regularized and regularized quasiparticle energies in the two regions of interest for $\eta = 0.1$, 1, and 10. It clearly shows how the regularization of the GW self-energy diabatically linked the two solutions to get rid of the discontinuities. However, this diabatization is more or less accurate depending on the value of η . For $\eta = 10$, the value is clearly too large inducing a large difference between the two sets of quasiparticle energies (purple curves). For $\eta = 0.1$, we have the opposite scenario where η is too small and some irregularities remain (green curves). We have found that $\eta = 1$ is a good compromise that does not alter significantly the quasiparticle energies while providing a smooth transition between the

two solutions. This value can be certainly refined for specific applications.

To further evidence this, Fig. 4 reports the difference between regularized (computed at $\eta = 1$) and non-regularized quasiparticle energies as functions of R_{H-H} for each orbital. The principal observation is that, in the absence of intruder states, the regularization induces an error below 10 meV for the HOMO ($p=1$) and LUMO ($p=2$), which is practically viable. Of course, in the troublesome regions ($p=3$ and $p=4$), the correction brought by the regularization procedure is larger (as it should) but it has the undeniable advantage to provide smooth curves.

As a final example, we report in Fig. 5 the ground-state potential energy surface of the F_2 molecule obtained at various levels of theory with the cc-pVDZ basis. In particular, we compute, with and without regularization, the total energy at the Bethe-Salpeter equation (BSE) level^{16,111-113} within the adiabatic connection fluctuation dissipation formalism^{39,114,115} following the same protocol detailed in Ref. 39. These results are compared to high-level coupled-cluster calculations^{116,117} extracted from the same work. As already shown in Ref. 39, the potential energy surface of F_2 at the BSE@ $G_0W_0@HF$ (blue curve) is very “bumpy” around the equilibrium bond length and it is clear that the regularization scheme (black curve computed with $\eta = 1$) allows to smooth it out without significantly altering the overall accuracy. Moreover, while it is extremely challenging to perform self-consistent GW calculations with-

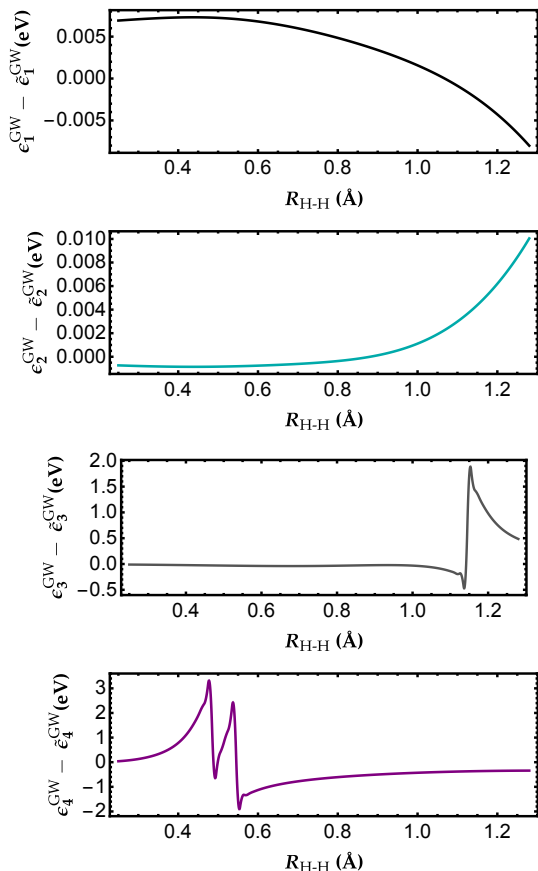


FIG. 4. Difference between regularized and non-regularized quasiparticle energies $\tilde{\epsilon}_p^{GW} - \epsilon_p^{GW}$ computed with $\eta = 1$ as functions of the internuclear distance R_{H-H} (in \AA) of H_2 at the $G_0W_0@HF/6-31G$ level.

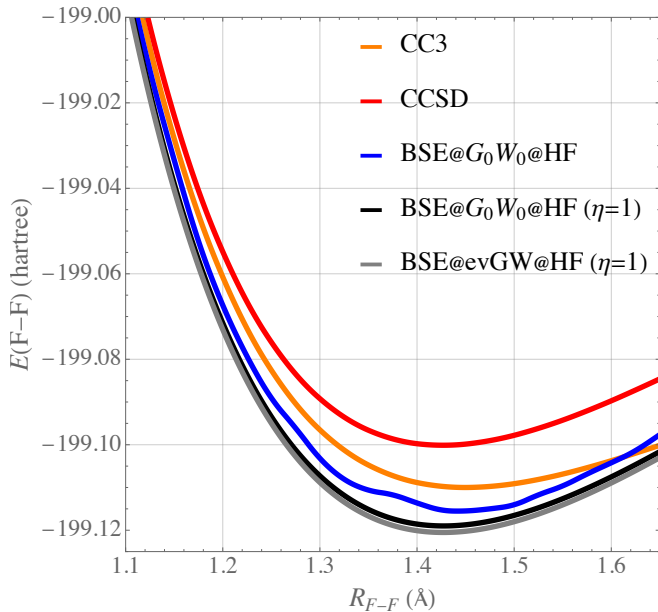


FIG. 5. Ground-state potential energy surface of F_2 around its equilibrium geometry obtained at various levels of theory with the cc-pVDZ basis set.

out regularization, it is now straightforward to compute the $BSE@evGW@HF$ potential energy surface (gray curve).

VI. CONCLUDING REMARKS

In the present article, we have provided mathematical and physical explanations behind the appearance of multiple solutions and discontinuities in various physical quantities computed within the GW approximation. More precisely, we have evidenced that intruder states are the main cause behind these issues and that this downfall of GW is a key signature of strong correlation. A simple and efficient regularization procedure inspired by the similarity renormalization group has been proposed to remove these discontinuities without altering too much the quasiparticle energies. Moreover, this regularization of the self-energy significantly speeds up the convergence of (partially) self-consistent GW methods. We hope that these new physical insights and technical developments will broaden the applicability of Green's function methods in the molecular electronic structure community and beyond.

ACKNOWLEDGMENTS

The authors thank Pina Romaniello and Xavier Blase for insightful discussions. This project has received funding from the European Research Council (ERC) under the European Union's Horizon 2020 research and innovation programme (Grant agreement No. 863481).

DATA AVAILABILITY STATEMENT

The data that supports the findings of this study are available within the article.

- ¹L. Hedin, *Phys. Rev.* **139**, A796 (1965).
- ²R. M. Martin, L. Reining, and D. M. Ceperley, *Interacting Electrons: Theory and Computational Approaches* (Cambridge University Press, 2016).
- ³F. Aryasetiawan and O. Gunnarsson, *Rep. Prog. Phys.* **61**, 237 (1998).
- ⁴G. Onida, L. Reining, and A. Rubio, *Rev. Mod. Phys.* **74**, 601 (2002).
- ⁵L. Reining, *Wiley Interdiscip. Rev. Comput. Mol. Sci.* **8**, e1344 (2017).
- ⁶D. Golze, M. Dvorak, and P. Rinke, *Front. Chem.* **7**, 377 (2019).
- ⁷S.-H. Ke, *Phys. Rev. B* **84**, 205415 (2011).
- ⁸F. Bruneval, *J. Chem. Phys.* **136**, 194107 (2012).
- ⁹F. Bruneval and M. A. L. Marques, *J. Chem. Theory Comput.* **9**, 324 (2013).
- ¹⁰F. Bruneval, S. M. Hamed, and J. B. Neaton, *J. Chem. Phys.* **142**, 244101 (2015).
- ¹¹X. Blase, P. Boulanger, F. Bruneval, M. Fernandez-Serra, and I. Duchemin, *J. Chem. Phys.* **144**, 034109 (2016).
- ¹²F. Bruneval, T. Rangel, S. M. Hamed, M. Shao, C. Yang, and J. B. Neaton, *Comput. Phys. Commun.* **208**, 149 (2016).
- ¹³F. Bruneval, *J. Chem. Phys.* **145**, 234110 (2016).
- ¹⁴P. Koval, D. Foerster, and D. Sánchez-Portal, *Phys. Rev. B* **89**, 155417 (2014).
- ¹⁵L. Hung, F. H. da Jornada, J. Souto-Casares, J. R. Chelikowsky, S. G. Louie, and S. Ögüt, *Phys. Rev. B* **94**, 085125 (2016).
- ¹⁶X. Blase, I. Duchemin, and D. Jacquemin, *Chem. Soc. Rev.* **47**, 1022 (2018).
- ¹⁷P. Boulanger, D. Jacquemin, I. Duchemin, and X. Blase, *J. Chem. Theory Comput.* **10**, 1212 (2014).

- ¹⁸J. Li, M. Holzmann, I. Duchemin, X. Blase, and V. Olevano, *Phys. Rev. Lett.* **118**, 163001 (2017).
- ¹⁹L. Hung, F. Bruneval, K. Baishya, and S. Ögüt, *J. Chem. Theory Comput.* **13**, 2135 (2017).
- ²⁰M. J. van Setten, F. Caruso, S. Sharifzadeh, X. Ren, M. Scheffler, F. Liu, J. Lischner, L. Lin, J. R. Deslippe, S. G. Louie, C. Yang, F. Weigend, J. B. Neaton, F. Evers, and P. Rinke, *J. Chem. Theory Comput.* **11**, 5665 (2015).
- ²¹M. J. van Setten, R. Costa, F. Viñes, and F. Illas, *J. Chem. Theory Comput.* **14**, 877 (2018).
- ²²E. Maggio, P. Liu, M. J. van Setten, and G. Kresse, *J. Chem. Theory Comput.* **13**, 635 (2017).
- ²³R. M. Richard, M. S. Marshall, O. Dolgouitcheva, J. V. Ortiz, J.-L. Brédas, N. Marom, and C. D. Sherrill, *J. Chem. Theory Comput.* **12**, 595 (2016).
- ²⁴L. Gallandi, N. Marom, P. Rinke, and T. Körzdörfer, *J. Chem. Theory Comput.* **12**, 605 (2016).
- ²⁵J. W. Knight, X. Wang, L. Gallandi, O. Dolgouitcheva, X. Ren, J. V. Ortiz, P. Rinke, T. Körzdörfer, and N. Marom, *J. Chem. Theory Comput.* **12**, 615 (2016).
- ²⁶O. Dolgouitcheva, M. Díaz-Tinoco, V. G. Zakrzewski, R. M. Richard, N. Marom, C. D. Sherrill, and J. V. Ortiz, *J. Chem. Theory Comput.* **12**, 627 (2016).
- ²⁷K. Krause, M. E. Harding, and W. Klopper, *Mol. Phys.* **113**, 1952 (2015).
- ²⁸M. Govoni and G. Galli, *J. Chem. Theory Comput.* **14**, 1895 (2018).
- ²⁹F. Caruso, M. Dauth, M. J. van Setten, and P. Rinke, *J. Chem. Theory Comput.* **12**, 5076 (2016).
- ³⁰D. Foerster, P. Koval, and D. Sánchez-Portal, *J. Chem. Phys.* **135**, 074105 (2011).
- ³¹P. Liu, M. Kaltak, J. c. v. Klimeš, and G. Kresse, *Phys. Rev. B* **94**, 165109 (2016).
- ³²J. Wilhelm, D. Golze, L. Talirz, J. Hutter, and C. A. Pignedoli, *J. Phys. Chem. Lett.* **9**, 306 (2018).
- ³³A. Förster and L. Visscher, *Front. Chem.* **9**, 736591 (2021).
- ³⁴I. Duchemin and X. Blase, *J. Chem. Theory Comput.* **17**, 2383 (2021).
- ³⁵S. Körbel, P. Boulanger, I. Duchemin, X. Blase, M. A. L. Marques, and S. Botti, *J. Chem. Theory Comput.* **10**, 3934 (2014).
- ³⁶F. Bruneval, N. Dattani, and M. J. van Setten, *Front. Chem.* **9**, 749779 (2021).
- ³⁷P. F. Loos, P. Romaniello, and J. A. Berger, *J. Chem. Theory Comput.* **14**, 3071 (2018).
- ³⁸M. Véril, P. Romaniello, J. A. Berger, and P. F. Loos, *J. Chem. Theory Comput.* **14**, 5220 (2018).
- ³⁹P.-F. Loos, A. Scemama, I. Duchemin, D. Jacquemin, and X. Blase, *J. Phys. Chem. Lett.* **11**, 3536 (2020).
- ⁴⁰J. A. Berger, P.-F. Loos, and P. Romaniello, *J. Chem. Theory Comput.* **17**, 191 (2020).
- ⁴¹S. Di Sabatino, P.-F. Loos, and P. Romaniello, *Front. Chem.* **9**, 751054 (2021).
- ⁴²M. Seidl, *Phys. Rev. A* **75**, 062506 (2007).
- ⁴³P. F. Loos and P. M. W. Gill, *Phys. Rev. A* **79**, 062517 (2009).
- ⁴⁴P. F. Loos and P. M. W. Gill, *Phys. Rev. Lett.* **103**, 123008 (2009).
- ⁴⁵I. Duchemin and X. Blase, *J. Chem. Theory Comput.* **16**, 1742 (2020).
- ⁴⁶D. Golze, J. Wilhelm, M. J. van Setten, and P. Rinke, *J. Chem. Theory Comput.* **14**, 4856 (2018).
- ⁴⁷D. Golze, L. Keller, and P. Rinke, *J. Phys. Chem. Lett.* **11**, 1840 (2020).
- ⁴⁸P. Pulay, *Chem. Phys. Lett.* **73**, 393 (1980).
- ⁴⁹P. Pulay, *J. Comput. Chem.* **3**, 556 (1982).
- ⁵⁰P. Romaniello, F. Bechstedt, and L. Reining, *Phys. Rev. B* **85**, 155131 (2012).
- ⁵¹D. Zhang, N. Q. Su, and W. Yang, *J. Phys. Chem. Lett.* **8**, 3223 (2017).
- ⁵²J. Li, Z. Chen, and W. Yang, *J. Phys. Chem. Lett.* **12**, 6203 (2021).
- ⁵³P.-F. Loos and P. Romaniello, “Static and dynamic bethe-salpeter equations in the t -matrix approximation,” (2022), [arXiv:2202.07936 \[physics.chem-ph\]](https://arxiv.org/abs/2202.07936).
- ⁵⁴A. Szabo and N. S. Ostlund, *Modern quantum chemistry* (McGraw-Hill, New York, 1989).
- ⁵⁵M. E. Casida and D. P. Chong, *Phys. Rev. A* **40**, 4837 (1989).
- ⁵⁶M. E. Casida and D. P. Chong, *Phys. Rev. A* **44**, 5773 (1991).
- ⁵⁷G. Stefanucci and R. van Leeuwen, *Nonequilibrium Many-Body Theory of Quantum Systems: A Modern Introduction* (Cambridge University Press, Cambridge, 2013).
- ⁵⁸J. V. Ortiz, *Wiley Interdiscip. Rev. Comput. Mol. Sci.* **3**, 123 (2013).
- ⁵⁹J. J. Phillips and D. Zgid, *J. Chem. Phys.* **140**, 241101 (2014).
- ⁶⁰J. J. Phillips, A. A. Kananenka, and D. Zgid, *J. Chem. Phys.* **142**, 194108 (2015).
- ⁶¹A. A. Rusakov, J. J. Phillips, and D. Zgid, *J. Chem. Phys.* **141**, 194105 (2014).
- ⁶²A. A. Rusakov and D. Zgid, *J. Chem. Phys.* **144**, 054106 (2016).
- ⁶³S. Hirata, M. R. Hermes, J. Simons, and J. V. Ortiz, *J. Chem. Theory Comput.* **11**, 1595 (2015).
- ⁶⁴S. Hirata, A. E. Doran, P. J. Knowles, and J. V. Ortiz, *J. Chem. Phys.* **147**, 044108 (2017).
- ⁶⁵M. S. Hybertsen and S. G. Louie, *Phys. Rev. B* **34**, 5390 (1986).
- ⁶⁶L. Hedin, *J. Phys.: Cond. Mat.* **11**, R489 (1999).
- ⁶⁷F. Bruneval, N. Vast, and L. Reining, *Phys. Rev. B* **74**, 045102 (2006).
- ⁶⁸A. Stan, N. E. Dahlen, and R. van Leeuwen, *Europhys. Lett. EPL* **76**, 298 (2006).
- ⁶⁹A. Stan, N. E. Dahlen, and R. van Leeuwen, *J. Chem. Phys.* **130**, 114105 (2009).
- ⁷⁰C. Rostgaard, K. W. Jacobsen, and K. S. Thygesen, *Phys. Rev. B* **81**, 085103 (2010).
- ⁷¹F. Caruso, P. Rinke, X. Ren, M. Scheffler, and A. Rubio, *Phys. Rev. B* **86**, 081102(R) (2012).
- ⁷²F. Caruso, D. R. Rohr, M. Hellgren, X. Ren, P. Rinke, A. Rubio, and M. Scheffler, *Phys. Rev. Lett.* **110**, 146403 (2013).
- ⁷³F. Caruso, P. Rinke, X. Ren, A. Rubio, and M. Scheffler, *Phys. Rev. B* **88**, 075105 (2013).
- ⁷⁴F. Caruso, *Self-Consistent GW Approach for the Unified Description of Ground and Excited States of Finite Systems*, PhD Thesis, Freie Universität Berlin (2013).
- ⁷⁵S. J. Bintrim and T. C. Berkelbach, *J. Chem. Phys.* **154**, 041101 (2021).
- ⁷⁶J. Lee and M. Head-Gordon, *J. Chem. Theory Comput.*, ASAP article (2018).
- ⁷⁷F. A. Evangelista, *J. Chem. Phys.* **141**, 054109 (2014).
- ⁷⁸G. Strinati, H. J. Mattausch, and W. Hanke, *Phys. Rev. Lett.* **45**, 290 (1980).
- ⁷⁹M. S. Hybertsen and S. G. Louie, *Phys. Rev. Lett.* **55**, 1418 (1985).
- ⁸⁰R. W. Godby, M. Schlüter, and L. J. Sham, *Phys. Rev. B* **37**, 10159 (1988).
- ⁸¹W. von der Linden and P. Horsch, *Phys. Rev. B* **37**, 8351 (1988).
- ⁸²J. E. Northrup, M. S. Hybertsen, and S. G. Louie, *Phys. Rev. Lett.* **66**, 500 (1991).
- ⁸³X. Blase, X. Zhu, and S. G. Louie, *Phys. Rev. B* **49**, 4973 (1994).
- ⁸⁴M. Rohlfing, P. Krüger, and J. Pollmann, *Phys. Rev. B* **52**, 1905 (1995).
- ⁸⁵M. Shishkin and G. Kresse, *Phys. Rev. B* **75**, 235102 (2007).
- ⁸⁶X. Blase and C. Attaccalite, *Appl. Phys. Lett.* **99**, 171909 (2011).
- ⁸⁷C. Faber, C. Attaccalite, V. Olevano, E. Runge, and X. Blase, *Phys. Rev. B* **83**, 115123 (2011).
- ⁸⁸T. Rangel, S. M. Hamed, F. Bruneval, and J. B. Neaton, *J. Chem. Theory Comput.* **12**, 2834 (2016).
- ⁸⁹X. Gui, C. Holzer, and W. Klopper, *J. Chem. Theory Comput.* **14**, 2127 (2018).
- ⁹⁰S. V. Faleev, M. van Schilfhaarde, and T. Kotani, *Phys. Rev. Lett.* **93**, 126406 (2004).
- ⁹¹M. van Schilfhaarde, T. Kotani, and S. Faleev, *Phys. Rev. Lett.* **96**, 226402 (2006).
- ⁹²T. Kotani, M. van Schilfhaarde, and S. V. Faleev, *Phys. Rev. B* **76**, 165106 (2007).
- ⁹³F. Kaplan, M. E. Harding, C. Seiler, F. Weigend, F. Evers, and M. J. van Setten, *J. Chem. Theory Comput.* **12**, 2528 (2016).
- ⁹⁴P. C. Martin and J. Schwinger, *Phys. Rev.* **115**, 1342 (1959).
- ⁹⁵G. Baym and L. P. Kadanoff, *Phys. Rev.* **124**, 287 (1961).
- ⁹⁶G. Baym, *Phys. Rev.* **127**, 1391 (1962).
- ⁹⁷O. J. Backhouse, M. Nusspickel, and G. H. Booth, *J. Chem. Theory Comput.* **16**, 1090 (2020).
- ⁹⁸O. J. Backhouse and G. H. Booth, *J. Chem. Theory Comput.* **16**, 6294 (2020).
- ⁹⁹O. J. Backhouse, A. Santana-Bonilla, and G. H. Booth, *J. Phys. Chem. Lett.* **12**, 7650 (2021).
- ¹⁰⁰G. Riva, T. Audinet, M. Vladaj, P. Romaniello, and J. A. Berger, “Photoemission spectral functions from the three-body green’s function,” (2022), [arXiv:2110.05623 \[cond-mat.str-el\]](https://arxiv.org/abs/2110.05623).
- ¹⁰¹M. Dvorak and P. Rinke, *Phys. Rev. B* **99**, 115134 (2019).

- ¹⁰²M. Dvorak, D. Golze, and P. Rinke, *Phys. Rev. Mat.* **3**, 070801(R) (2019).
- ¹⁰³P. F. Loos, “QuAcK: a software for emerging quantum electronic structure methods,” (2019), <https://github.com/pfloos/QuAcK>.
- ¹⁰⁴N. Forsberg and P.-Å. Malmqvist, *Chem. Phys. Lett.* **274**, 196 (1997).
- ¹⁰⁵J. Shee, M. Loipersberger, A. Rettig, J. Lee, and M. Head-Gordon, *J. Phys. Chem. Lett.* **12**, 12084 (2021).
- ¹⁰⁶F. Wegner, *Ann. Phys. Leipzig* **3**, 77 (1994).
- ¹⁰⁷S. D. Glazek and K. G. Wilson, *Phys. Rev. D* **49**, 4214 (1994).
- ¹⁰⁸S. R. White, *J. Chem. Phys.* **117**, 7472 (2002).
- ¹⁰⁹F. A. Evangelista, *J. Chem. Phys.* **140**, 124114 (2014).
- ¹¹⁰C. Li and F. A. Evangelista, *Annu. Rev. Phys. Chem.* **70**, 245 (2019).
- ¹¹¹E. E. Salpeter and H. A. Bethe, *Phys. Rev.* **84**, 1232 (1951).
- ¹¹²G. Strinati, *Riv. Nuovo Cimento* **11**, 1 (1988).
- ¹¹³X. Blase, I. Duchemin, D. Jacquemin, and P.-F. Loos, *J. Phys. Chem. Lett.* **11**, 7371 (2020).
- ¹¹⁴E. Maggio and G. Kresse, *Phys. Rev. B* **93**, 235113 (2016).
- ¹¹⁵C. Holzer, X. Gui, M. E. Harding, G. Kresse, T. Helgaker, and W. Klopper, *J. Chem. Phys.* **149**, 144106 (2018).
- ¹¹⁶G. P. Purvis III and R. J. Bartlett, *J. Chem. Phys.* **76**, 1910 (1982).
- ¹¹⁷O. Christiansen, H. Koch, and P. Jørgensen, *J. Chem. Phys.* **103**, 7429 (1995).